

FUZZY WITH GAN BASED MICROINVERTER WITH BOOST AND HALF BRIDGE INVERTER

¹Kanoori Jyothi Swarup, ²A.Ramakrishna

¹M.tech student, ²Associate Professor

Department of EEE

Bonam Venkata chalamayya Engineering Collage (A), East Godavari District

ABSTRACT

Due to their plug and play feature, easy installation, and higher power yield under partial shading conditions, microinverters have gained popularity in the roof-top-PV market. This paper explores a converter system for the transformer-less microinverter with coupled inductor based interleaved boost as the dc-dc stage and half bridge voltage swing (HBVS) inverter with induction motor by using fuzzy logic as the dc-ac stage. The dc-dc stage is capable of offering high gain with a flexible choice of turns ratio of the coupled inductor but simultaneously maintaining a reduced voltage stress on the main switch. The HBVS inverter has the advantages of reduced capacitor requirement for 120 Hz power decoupling and being half-bridge derived, minimized capacitive-coupled common-mode ground currents. A 300 W GaN based inverter prototype with 30 V nominal dc input and 120 V, 60 Hz nominal ac output and operating at switching frequency of 200/100 kHz has been developed.

I. INTRODUCTION

Photovoltaic (PV) inverters form the backbone of both utility and residential grid-connected PV systems. Recently, in such applications micro inverters are increasingly grabbing more market share due to its easy installation, plug and play concept, and higher power yield under partial shading condition. As they are directly connected to each of the PV panel, typically the input voltage for such inverters spans from 30 to 40 V, whereas, to interface to the grid the ac output voltage needs to be 120 V/ 230 V RMS. This necessitates a high voltage boost for interfacing a PV panel to the grid. Thus most of the commercialized micro inverters are implemented with high frequency transformer isolation providing higher voltage step-up through the turns ratio accommodation as is done in . However, transformer-less versions are preferred because of their advantages in higher efficiency, reduced volume, and lower cost with the removal of lossy and bulky transformer. Authors in have proposed non-isolated high gain boost converters which are also suitable to implement as the high gain

stage of transformer-less microinverter applications. The other two challenges encountered by any transformer-less microinverters are similar to that of any PV string inverters implemented without isolation. These include the mitigation of the capacitively coupled ground current arising from the parasitic capacitance between the PV panel and grid neutral and similar to any other single phase rectifiers and inverters, the need to support double line frequency power decoupling with reliable and efficient film capacitors. In this paper, a converter system for the transformer less micro inverter with coupled inductor based interleaved boost as the dc-dc stage and half bridge voltage swing (HBVS) inverter as the dc-ac stage is proposed. The dc-dc stage has two interleaved phases and is capable of offering high gain with a flexible choice of turns ratio of the coupled inductor but simultaneously maintaining a reduced voltage stress on the main switches of both the phases. Additionally, the inductor current is interleaved, reducing the equivalent ripple on the converter input current and the inductor core loss and high frequency copper loss. The HBVS inverter has the advantages of connecting the PV negative terminal to the grid neutral through line frequency varying half bridge capacitor, thereby eliminating the capacitive-coupled common-mode ground currents, critical for all transformer-less PV inverters. Also through sinusoidal variation of the half bridge capacitor voltage along with a limited ripple on the dclink, the decoupling capacitor is reduced allowing an all-film capacitor implementation.

II. LITERATURE SURVEY:

This proposes a novel high voltage-gain LLC micro-converter for PV applications. The converter has simple structure and minimum components with low cost. It can realize high voltage gain based on the voltage doubler rectifier with the optimal turns ratio. The main power switches can achieve ZVS and the output diodes can realize ZCS in wide input and load range. By utilizing the voltage doubler in the secondary side, the voltage stress over the output diodes can be reduced by half compared to the conventional center-tapped full-wave rectifier. A 24-48 V input, 380 V output and 200W prototype

was built to verify the benefits of the proposed converter. The achieved efficiency of the converter peaks at 96.6% and the CEC weighted efficiency reaches 95.4% .

Modelling and control design of paralleled DC-DC switching converters Power electronic systems are widely used today to provide power processing for applications ranging from computing and communications to medical electronics, appliance control, transportation, and high-power transmission. The associated power levels range from milli watts to megawatts. These systems typically involve switching circuits composed of semiconductor switches such as thyristors, MOSFETs, and diodes, along with passive elements such as inductors, capacitors, and resistors, and integrated circuits for control. Application of Kalman filters in model-based fault diagnosis of a DC-DC boost converter

III. PHOTOVOLTAIC CELL

A PV cell is a simple p-n junction diode that converts the irradiation into electricity. Fig.1 illustrates a simple equivalent circuit diagram of a PV cell. This model consists of a current source which represents the generated current from PV cell, a diode in parallel with the current source, a shunt resistance, and a series resistance.

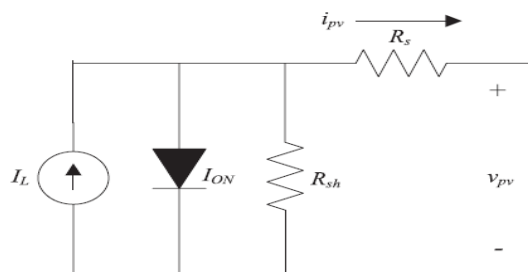


Fig.1 Equivalent circuit diagram of the PV cell

IV.FUZZY

In recent years, the number and variety of applications of fuzzy logic have increased significantly. The applications range from consumer products such as cameras, camcorders, washing machines, and microwave ovens to industrial process control, medical instrumentation, decision support systems, and portfolio selection. To understand why use of fuzzy logic has grown, you must first understand what is meant by fuzzy logic.

Fuzzy logic has two different meanings. In a narrow sense, fuzzy logic is a logical system, which is an extension of multivalve logic. However, in a wider sense fuzzy logic (FL) is almost synonymous with the theory of fuzzy sets, a theory which relates to classes of objects with un sharp boundaries in which membership is a matter of degree. In this perspective, fuzzy logic in its narrow sense is a branch of FL. Even in its more narrow definition,

fuzzy logic differs both in concept and substance from traditional multivalve logical systems.

In fuzzy Logic Toolbox software, fuzzy logic should be interpreted as FL, that is, fuzzy logic in its wide sense. The basic ideas underlying FL are explained very clearly and insightfully in Foundations of Fuzzy Logic. What might be added is that the basic concept underlying FL is that of a linguistic variable, that is, a variable whose values are words rather than numbers. In effect, much of FL may be viewed as a methodology for computing with words rather than numbers. Although words are inherently less precise than numbers, their use is closer to human intuition. Furthermore, computing with words exploits the tolerance for imprecision and thereby lowers the cost of solution.

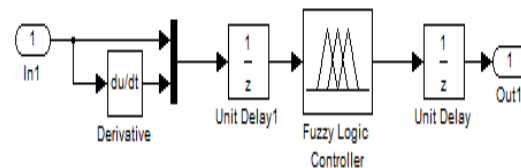


Fig.2 Fuzzy interference system

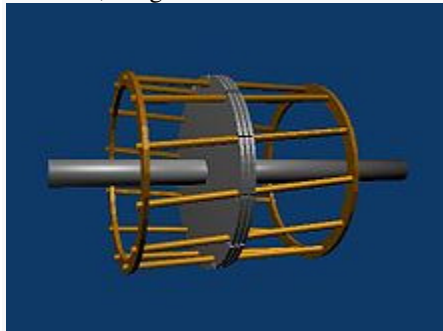
V.INDUCTION MOTOR

An induction motor or asynchronous motor is an AC electric motor in which the electric current in the rotor needed to produce torque is obtained by electromagnetic induction from the magnetic field of the stator winding.^[1] An induction motor can therefore be made without electrical connections to the rotor.^[a] An induction motor's rotor can be either wound type or squirrel-cage type.

Three-phase squirrel-cage induction motors are widely used as industrial drives because they are rugged, reliable and economical. Single-phase induction motors are used extensively for smaller loads, such as household appliances like fans. Although traditionally used in fixed-speed service, induction motors are increasingly being used with variable-frequency drives (VFDs) in variable-speed service. VFDs offer especially important energy savings opportunities for existing and prospective induction motors in variable-torque centrifugal fan, pump and compressor load applications. Squirrel cage induction motors are very widely used in both fixed-speed and variable-frequency drive (VFD) applications.



A model of Tesla's first induction motor, in Tesla Museum, Belgrade



Squirrel cage rotor construction, showing only the center three laminations

VI. PROPOSED AND CONTROL DESIGN

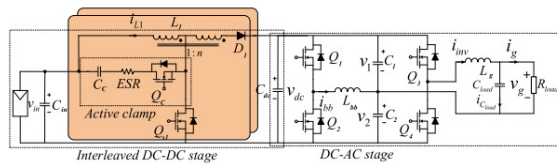


Fig3: Proposed Simulation diagram

Fig.3 shows the coupled inductor based interleaved boost followed by HBVS inverter considered for the transformer-less microinverter application. The high gain dc-dc stage is realized by coupled inductor with two interleaved phases, whereas, the dc-ac stage offers an active power decoupling approach with a large sinusoidal swing of the half bridge capacitors with a limited 120 Hz ripple on the dc-link to minimize the decoupling capacitor requirement. It also mitigates the capacitive ground current. Also the topological variation offers connecting the grid neutral directly to the PV negative terminal through half bridge capacitor, which mitigates the capacitive ground current.

A. Coupled inductor interleaved boost

Fig.4 shows the circuit schematic of the coupled inductor interleaved boost converter for providing high voltage gain. In the present application, two interleaved phases are considered to scale the power. They process power in parallel. Each phase is comprised of the active switch Q_s , diode D , and coupled inductor L with turns ratio $1 : n$ as shown.. Fig. 4 gives the input current (i_{in}) and

primary and secondary side coupled inductor current for both the interleaved phases assuming ideal coupling under continuous conduction mode (CCM) condition. The converter gain (k) is a function of the coupled inductor turns ratio n as given in (1).

$$k = \frac{V_o}{V_{in}} = \frac{i_{L1} + i_{L2}}{i_o} = 1 + nD \quad (1)$$

The MOSFET and diode voltage stress of the main circuit are given in (2), which shows that the stress on the MOSFET (V_{swm}) is significantly reduced, thus lower voltage rating switch with lower ON-resistance $R_{DS(ON)}$ (which almost varies proportionally with the square of the blocking-voltage) can be used, reducing the corresponding conduction loss. However, the diode voltage stress ($V_{diode m}$) is in fact higher than the conventional boost. But it would not affect the converter efficiency as the SiC diode forward voltage drop does not scale remarkably with the voltage rating and diode current is significantly lower than the main switch current.

$$V_{swm} = V_o + nV_{in} \frac{1}{1+n}; \quad V_{diode m} = V_o + nV_{in} \quad (2)$$

For practical implementation the primary and secondary windings of the coupled inductor would not be ideally coupled introducing leakage path in the switching circuit, voltage oscillation, and power dissipation. Thus an active clamp is used here to ensure the recycling of the leakage. On the main switch. But this introduces an additional active switch, the associated gate driver circuitry, and corresponding loss in the driving circuit. Q_c and C_c constitute the active clamp circuit for each phase. Q_c is operated in complementary to Q_s with appropriate dead-time.

B. Half bridge voltage swing inverter

The output from the dc-dc stage v_{dc} gets connected to the HBVS inverter stage as its input. The dc-ac stage is comprised of a synchronous buck-boost stage followed by a half bridge inverter. The grid neutral is directly connected to the PV negative terminal through half bridge capacitor, which mitigates the capacitive ground current, a critical requirement for transformer-less PV inverters.

The grid voltage and grid current at an arbitrary power factor $\cos \theta$, with the corresponding instantaneous grid power are given in (3)

$$v_g = V_g \sin(\omega t); \quad i_g = I_g \sin(\omega t + \theta) \quad P_g = V_g I_g \frac{1}{2} (\cos \theta - \cos(2\omega t + \theta)) \quad (3)$$

As P_g has 2ω ripple component and power from PV is a pure dc, the instantaneous power from input is not equal to that of the output and energy storage element is required to ensure power decoupling i.e., instantaneous power balance. In this converter a large sinusoidal swing of the half-bridge capacitors v_1 and v_2 [expressions are given in (4)] are allowed along with a limited double line frequency

voltage ripple on the dc-link v_3 [given in (5)] to address the power decoupling with a reduced capacitor value.

$$v_1 = v_3 \sqrt{2} + A \sin(\omega t + \zeta); v_2 = v_3 \sqrt{2} - A \sin(\omega t + \zeta) \quad (4)$$

$$v_{dc} = V + V_r \sin(2\omega t + \theta) \quad (5)$$

where, $2A$ is the allowed peak-peak ripple of the halfbridge capacitor voltages, ζ is their phase shift relative to the grid voltage, V is the dc-link average voltage, and V_r is the amplitude of dc-link ripple voltage. The ripple power P_i supported by any capacitor C_i is given in (6).

$$P_i = \frac{1}{2} \frac{d}{dt} C_i v_i^2 \quad (6)$$

Using (6), the total ripple power supported by all the three capacitors C_1 , C_2 , and C_{dc} can be computed [20] which is $P_t = P_1 + P_2 + P_{dc}$. By comparing the magnitude and phase of $2\omega t$ terms in P_g and P_t , the condition for double line frequency power decoupling as given in (7) is obtained.

$$V V_r (2C_{dc} + C) + CA^2 = V_g I_g \sqrt{2} \omega = S_g \omega \zeta = \pi \sqrt{4 + \theta^2} \quad (7)$$

Further, in order to regulate the grid current and voltage without distortion, the condition given in (8) needs to be satisfied instantaneously ensuring that the converter is not over-modulated at any operating interval. ($v_1 > v_g$ if $v_g \geq 0$ $v_2 > |v_g|$ if $v_g < 0$)

VII.SIMULATION RESULTS

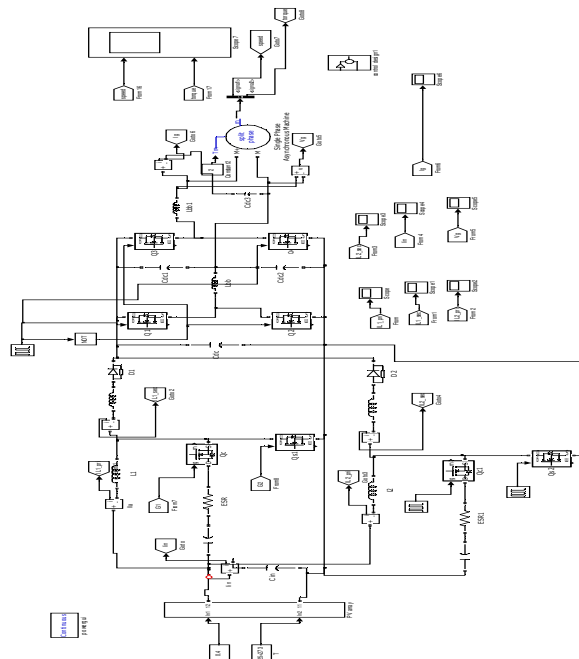


Fig4: Proposed Simulation diagram with fuzzy

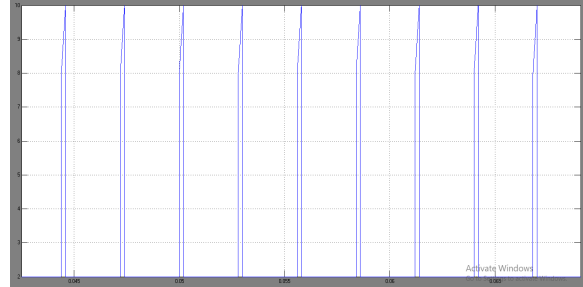


Fig5:L2-Primary currents

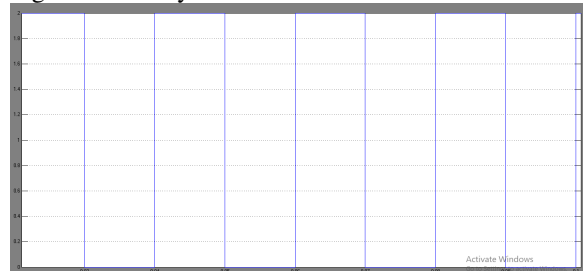


Fig6:L1: Secondary currents

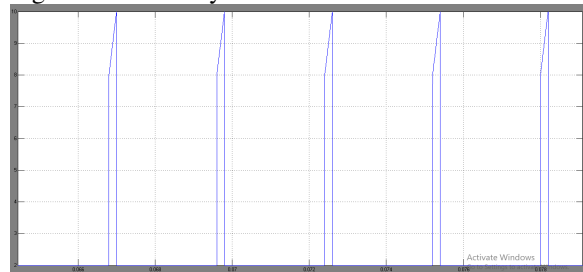


Fig7:L2: Primary currents

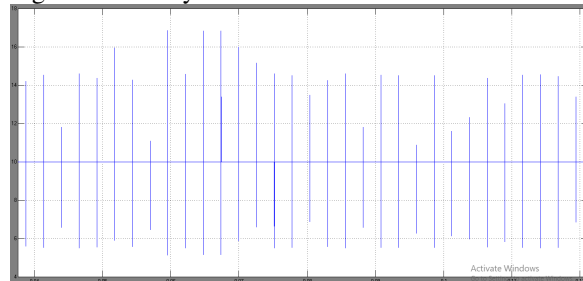


Fig8:Iin

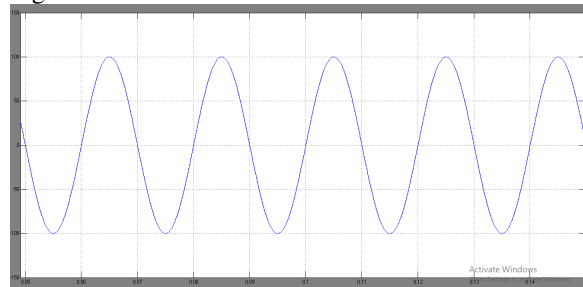


Fig9: Grid voltage

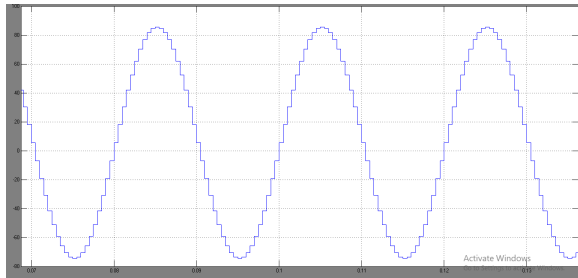


Fig10: Grid Currents

VIII. CONCLUSION

The project discusses a transformer-less micro inverter topology with fuzzy logic. The coupled inductor based interleaved boost dc-dc stage is capable of offering high gain with a flexible choice of turns ratio of the coupled inductor but simultaneously maintaining a reduced voltage stress on the main switch with fuzzy. The HBVS inverter dc-ac stage has the advantages of reduced capacitor requirement for 120 Hz power decoupling and being half-bridge derived, minimized capacitive-coupled common-mode ground currents. Simulation results are provided to validate its operation.

REFERENCES

- [1] H. D. Gui, Z. Zhang, X. F. He, and Y. F. Liu, "A high voltage-gain LLC micro-converter with high efficiency in wide input range for PV applications," in 2014 IEEE Applied Power Electronics Conference and Exposition - APEC 2014, March 2014, pp. 637–642.
- [2] J. Roy, Y. Xia, and R. Ayyanar, "Gan based transformer-less microinverter with extended-duty-ratio boost and doubly grounded voltage swing inverter," in 2017 IEEE Applied Power Electronics Conference and Exposition (APEC), March 2017, pp. 2970–2976.
- [3] M. Kasper, M. Ritz, D. Bortis, and J. W. Kolar, "PV panelintegrated high step-up high efficiency isolated GaN DC-DC boost converter," in Telecommunications Energy Conference 'Smart Power and Efficiency' (INTELEC), Proceedings of 2013 35th International, Oct 2013, pp. 1–7.
- [4] N. Sukesh, M. Pahlevaninezhad, and P. K. Jain, "Analysis and implementation of a single-stage flyback PV microinverter with soft switching," IEEE Transactions on Industrial Electronics, vol. 61, no. 4, pp. 1819–1833, April 2014.
- [5] R. K. Surapaneni and A. K. Rathore, "A single-stage ccm zeta microinverter for solar photovoltaic ac module," IEEE Journal of Emerging and Selected Topics in Power Electronics, vol. 3, no. 4, pp. 892–900, Dec 2015.
- [6] J. Roy and R. Ayyanar, "Seamless transition of the operating zones for the extended-duty-ratio boost converter," in 2017 IEEE Energy Conversion

Congress and Exposition (ECCE), Oct 2017, pp. 4920–4926.

[7] L. H. S. C. Barreto, P. P. Praa, D. S. Oliveira, and R. N. A. L. Silva, "High-voltage gain boost converter based on three-state commutation cell for battery charging using PV panels in a single conversion stage," IEEE Transactions on Power Electronics, vol. 29, no. 1, pp. 150–158, Jan 2014.

[8] J. Roy and R. Ayyanar, "Gan based high gain non-isolated dc-dc stage of microinverter with extended-duty-ratio boost," in 2016 IEEE Energy Conversion Congress and Exposition (ECCE), Sept 2016, pp. 1–8.

[9] N. Zhang, D. Sutanto, K. M. Muttaqi, B. Zhang, and D. Qiu, "High-voltage-gain quadratic boost converter with voltage multiplier," IET Power Electronics, vol. 8, no. 12, pp. 2511–2519, 2015.

[10] J. Roy and R. Ayyanar, "Sensor-less current sharing over wide operating range for extended-duty-ratio boost converter," IEEE Transactions on Power Electronics, vol. 32, no. 11, pp. 8763– 8777, Nov 2017.